17) Ladage PM, Yamamoto K, Li L, Ren DH et al : Corneal epithelial homeostasis following daily and overnight contact lens wear. Contact Lens & Anterior Eye 25：11-21, 2002.
18) O'Leary DJ, Madgewick R, Wallace J & Ang J : Size and number of epithelial cells washed from the cornea after contact lens wear. Optom Vis Sci 75：692-696, 1998.
19) Miller MJ, Callahan DE, McGrath D, Manchester R et al : Disinfection efficacy of contact lens care solutions against ocular pathogens. CLAO J 27：16-22, 2001.
20) 柳井亮二，植田喜一，田尻大治，松本 融他：アカントアメーバおよびウイルスに対するポビドンヨード製剤の有効性．日コレ誌 47：37-41, 2005.
21) Beattie TK, Tomlinson A & Seal DV : Surface treatment or material characteristic : The reason for the high level of *Acanthamoeba* attachment to silicone hydrogel contact lenses. Eye & Contact Lens 29：S40-S43, 2003.
22) 穂積和弘，針谷明美，伊勢ノ海一之，松澤亜紀子他：終日装用におけるシリコーンハイドロゲルレンズとハイドロゲルレンズとの付着細菌，付着タンパク質および結膜嚢細菌叢の比較検討．日コレ誌 49：26-30, 2007.

(2011年8月9日受付)

筆頭著者
稲葉 昌丸

稲葉眼科

OPEN ACCESS Freely available online

PLoS one

Gibberellin Biosynthetic Inhibitors Make Human Malaria Parasite *Plasmodium falciparum* Cells Swell and Rupture to Death

Tomoko Toyama[1,2*¤], Michiru Tahara[3], Kisaburo Nagamune[3], Kenji Arimitsu[4], Yoshio Hamashima[4], Nirianne M. Q. Palacpac[2], Hiroshi Kawaide[5], Toshihiro Horii[2], Kazuyuki Tanabe[1,2*]

1 Laboratory of Malariology, Research Institute for Microbial Diseases, Osaka University, Yamadaoka, Suita, Osaka, Japan, **2** Department of Molecular Protozoology, Research Institute for Microbial Diseases, Osaka University, Yamadaoka, Suita, Osaka, Japan, **3** Department of Parasitology, National Institute of Infectious Diseases, Toyama, Shinjuku-ku, Tokyo, Japan, **4** Pharmaceutical Manufacturing Chemistry, Division of Medicinal Chemical Sciences, Kyoto Pharmaceutical University, Misasagi-Nakauchicho, Yamashinaku, Kyoto, Japan, **5** Institute of Agriculture, Tokyo University of Agriculture and Technology (TUAT), Saiwaicho, Fuchu, Tokyo, Japan

Abstract

Malaria remains as one of the most devastating infectious disease, and continues to exact an enormous toll in medical cost and days of labor lost especially in the tropics. Effective malaria control and eventual eradication remain a huge challenge, with efficacious antimalarials as important intervention/management tool. Clearly new alternative drugs that are more affordable and with fewer side effects are desirable. After preliminary *in vitro* assays with plant growth regulators and inhibitors, here, we focus on biosynthetic inhibitors of gibberellin, a plant hormone with many important roles in plant growth, and show their inhibitory effect on the growth of both apicomplexa, *Plasmodium falciparum* and *Toxoplasma gondii*. Treatment of *P. falciparum* cultures with the gibberellin biosynthetic inhibitors resulted in marked morphological changes that can be reversed to a certain degree under hyperosmotic environment. These unique observations suggest that changes in the parasite membrane permeability may explain the pleiotropic effects observed within the intracellular parasites.

Citation: Toyama T, Tahara M, Nagamune K, Arimitsu K, Hamashima Y, et al. (2012) Gibberellin Biosynthetic Inhibitors Make Human Malaria Parasite *Plasmodium falciparum* Cells Swell and Rupture to Death. PLoS ONE 7(3): e32246. doi:10.1371/journal.pone.0032246

Editor: Gordon Langsley, Institut national de la santé et de la recherche médicale - Institut Cochin, France

Received August 18, 2011; **Accepted** January 24, 2012; **Published** March 7, 2012

Funding: This work was supported by Ministry of Education, Culture, Sports, Science and Technology grant (#18073013) and the Japan Society for the Promotion of Science grant (#18GS03140013). The funders had no role in study design, data collection and analysis, decision to publish, or preparation of the manuscript.

Competing Interests: The authors have declared that no competing interests exist.

* E-mail: toyama-imhp@umin.ac.jp (TT); kztanabe@biken.osaka-u.ac.jp (KT)

¤ Current address: Department of Dermatology, Course of Integrated Medicine, Graduate School of Medicine, Osaka University, Yamadaoka, Suita, Osaka, Japan

Introduction

Malaria, caused by the genus *Plasmodium*, is one of the most common infections in the world responsible for about 1 million deaths per year. Artemisinin-based combination therapies (ACTs) are currently the first-line and only the best weapon against malaria [1]. Drug resistance, which rendered chloroquine and sulfadoxine-pyrimethamine infective for malaria control from 1970 to 1990s, remains as one of the greatest challenges facing malaria control today. Besides, ACT is 4 to 22× more expensive than common drugs and access is generally poor in African countries [2]. Also, although its clinical efficacy has not yet been compromised, there are recent reports that show the first evidence of artemisinin resistance [3]. Admittedly, the development of new inexpensive, effective and safe drugs with new mechanisms is strongly needed.

Plant-specific organelles and mechanisms in the phylum *Apicomplexa*, in which *Plasmodium* and other medically and veterinarily important pathogens are included, have been brought to focus as potential targets for new drugs since associated enzymes were found in plants and bacteria but not in animal metabolic pathways. Examples of these are plant-like vacuoles in parasite cells and the mevalonate-independent biosynthesis of isoprenoid in apicoplasts [4], [5]. The rationale was further strengthened with the demonstration that the apicoplast is essential for malaria parasite survival [6] and that metabolic pathways in the apicoplast are essential for parasite growth [7]. In addition, identification of inhibitors in these pathways might also result in synergistic drug combinations, which could have increased therapeutic value. The plant hormone abscisic acid (ABA) and ABA biosynthetic inhibitors have, likewise, been shown to affect parasite egress from infected host cells in *Toxoplasma gondii* [8].

In this study, we have preliminarily explored a wide variety of plant growth regulators, including plant hormones and corresponding inhibitors, to investigate their effect(s) on the growth of the most virulent human malaria parasite, *Plasmodium falciparum*. We have also used the apicomplexan parasite, *T. gondii* for comparison. *T. gondii* infects a broad spectrum of hosts and efficient drugs with low side effects and usable for human therapies are also highly needed. Plant growth inhibitors are commonly used in agriculture for years and have been synthesized in bulk, efficiently and cheaply, either naturally or artificially. Well-

established manufacturing methods and facilities, as well as their safety profile (toxicity and teratogenicity) in animals, crops and humans are also available. Thus, plant growth inhibitors showing anti-apicomplexan activities might give valuable clues for prophylactic or therapeutic reagents effective for infectious diseases caused by protozoan parasites.

Materials and Methods

Chemicals

AMO-1618 (2-isopropyl-4-dimethylamino-5-methyl-phenyl-1-piperidinecarboxylate methyl chloride) was obtained from CALBIOCHEM (La Jolla, USA). FC-907 [*N,N,N,*-trimethyl-1-methyl-(2′,6′,6′-trimethylcyclohex-2′-en-1′-yl)prop-2-enylammonium iodide] was kindly provided by Prof. Y. Kamiya (RIKEN, Japan). LysoTracker® Red DND-99 was obtained from Invitrogen (San Diego, USA). All other chemicals were purchased from Wako Pure Chemicals (Osaka, Japan).

Prior to use and dilution at various concentrations, AMO-1618, chlorocholine chloride, prohexadione and FC-907 were dissolved in distilled water. INA and ancymidol were dissolved in DMSO and diluted in 0.1% DMSO. Paclobutrazol and uniconazole P were dissolved in ethanol and diluted in the culture medium.

Enantiomeric resolution of racemic INA (Wako) was carried out by high performance liquid chromatography (HPLC; LC-908, Japan Analytical Industry Co., Ltd, Japan). Elution order of enantiomers was determined by an ultraviolet absorption detector (SPD-10A, Shimadzu, Japan) using Chiralcel OD column [25×0.46 cm, Daicel Chemical Industries, Japan, mobile phase: n-hexane-2-propanol (7:3, v/v), flow rate: 1.0 ml/min]. All resolutions were carried out at 26°C; detection at 275 nm. The assignment of the peaks was achieved by comparison with the synthesized (*S*)-form INA sample as previously described [9]: peak with shorter retention time correspond to the (*R*)-form and the peak with longer retention time to the (*S*)-form. Percentage purity of the products was calculated to be 97.0% and 99.5% for (*S*)- and (*R*)-forms, respectively, based on peak areas.

In vitro culture

P. falciparum strain 3D7 was cultured at 3% hematocrit in RPMI 1640 supplemented with 10% human serum, 50 mg/l hypoxanthine and 25 mg/l gentamicin, as previously described [10]. Cultures were maintained at 37°C in a gas mixture of 5% CO_2, 5% O_2, and 90% N_2.

The *T. gondii* strain 2F tachyzoites, derived from strain RH, constitutively expressing cytoplasmic β-galactosidase (β-gal), were routinely grown in Vero cells (African green monkey kidney, strain ATCC CCL-81^{TM}) at 37°C under 5% CO_2 in RPMI 1640 medium containing 10% fetal calf serum [11].

In vitro antimalarial assay of plant growth regulators

Asynchronous *P. falciparum* 3D7 was used. Various concentrations of compounds in appropriate solvents (water, ethanol or DMSO) were prepared and added to 12-well plates. Starting parasitemia was at 0.1% in 2.5 ml culture medium. Growth was assessed after 72 h by percentage parasitemia using thin blood smears. The number of parasitized erythrocytes over a total of 3,000 erythrocytes was examined. Drug-free control cultures were run simultaneously.

For *T. gondii* studies, confluent Vero cell cultures were incubated for 2 days and infected with 2.5×10^5 tachyzoites in RPMI 1640 medium containing 3% FCS using a 96-well plate. Tachyzoites were harvested after 2 days and β-gal activity was analyzed using a colorimetric assay [12].

Morphological effects of gibberellin biosynthetic inhibitors on P. falciparum

Tightly synchronized parasites within 4 h life span were prepared using 5% sorbitol treatment and percoll centrifugation. Synchronized parasites were treated with either 50 μM INA or 250 μM AMO-1618 from 0 h (ring), 20 h (immature trophozoite), 28 h (mature trophozoite) or 36 h (schizont). Giemsa-stained thin-blood smears were prepared after 4, 8 and 12 h treatment. Digital imaging was performed on a HC-300 (Fujifilm, Japan) and representative parasite images are shown.

Fluorescence Microscopy

Thin-blood smears of infected erythrocytes treated with INA were stained with acridine orange (100 μg/ml). Fluorescence microscopy and confocal imaging were carried out using the Axioplan 2 microscope (Zeiss, German) and SPOT PS-BW CCD camera (Seki Technotron Corp., Japan). Filter sets for green fluorescence (green: nucleoli; emission LP515, excitation BP 450–490) and red fluorescence (red: cytoplasm; emission LP590, excitation 546/12) were used. Nile Red staining was carried out by addition of 1 μg/ml dye to the culture medium 1 h prior to microscopic analysis. Nile Red was excited at 546 nm and emission detected above 590 nm. To stain with rhodamine 123 and LysoTracker® Red DND-99, 10 ng/ml rhodamine or 75 nM LysoTracker were added to the culture and incubated for 1 h. Confocal images were obtained with excitation above 546 nm and emission above 590 nm.

Electron microscopy

Intraerythrocytic parasites treated with 50 μM INA for 6 h, 250 μM AMO-1618 for 8 h or 0.1% DMSO for 6 h were centrifuged at 3500× g for 1 min and fixed in 2% glutaraldehyde in 1× PBS for 1 h. After washing in 1× PBS, fixed cells were treated as described [13]. Sections were viewed in a transmission electron microscope JEM-1011 (JEOL Ltd., Japan).

Effects of osmotic pressure on INA-treated P. falciparum

P. falciparum in RPMI 1640 containing 10% human serum was grown to 5–10% parasitemia and synchronized by sorbitol treatment. After 21 h, 0.9 ml of early trophozoite-stage parasites was mixed with 0.1 ml of 1×, 2×, 3× and 4× PBS and treated simultaneously with 50 μM INA or 0.1% DMSO for 8 h (INA stock solution was prepared as 50 mM in DMSO and diluted to 1/1000 for assay). Parasitemia was determined using Giemsa-stained thin smears by a laboratory technician blinded to treatment assignments. Each treatment was replicated thrice and experiments were performed twice.

Volumes of 0, 0.1, 0.2 and 0.4 ml sterilized water was adjusted to 0.4 ml by mixing with appropriate amounts of RPMI 1640 medium containing 10% human serum for the different dilution series. Hyposmotic media were mixed with 0.6 ml of *P. falciparum* culture synchronized to early-stage trophozoites.

GC-MS analysis of sterols in P. falciparum

Parasites were cultured in 5 ml RPMI 1640 supplemented with 1% serum free AlbuMAX® II (Invitrogen). Parasitized erythrocytes were collected by centrifugation and hemolyzed in 0.54 ml of 0.15% saponin in RPMI 1640. Erythrocyte-free parasites were washed twice with 4 ml of 1× PBS and suspended in 0.4 ml of 1× PBS. Geranylgeraniol at 50 μg was added to the suspension as an internal standard and extraction with 1 ml of chloroform was carried out 3 times by shaking the mixture at 37°C.

Chloroform extracts were pooled and 1 µl solution was directly injected into the GC-MS (gas chromatography/mass spectroscopy) instrument (JEOL; JMS-Bu25 GCMate: ionization energy at 70 eV, filament current at 300 mA) with a DB-5 capillary column [0.25 mm i.d.×15 m, film thickness of 0.25 mm (J&W Scientific, USA)]. The He carrier gas flow rate was 1 ml/min (constant flow), the injector temperature was 250°C, and the samples were introduced by splitless injection. After injection, the oven temperature program was held at 80°C for 1 min, then increased to 200°C at 30°C min^{-1}, followed by a further increase to 300°C at 15°C min^{-1} after which it was held constant at 300°C for 2 min.

For quantitative analysis, commercially available cholesterol and geranylgeraniol (Sigma) was detected by GC-MS and corresponding peaks were used as authentic standards for cholesterol and geranylgeraniol, respectively. Cholesterol was calculated based on ratio of peak areas with geranylgeraniol.

Results

Antimalarial activity of gibberellin biosynthetic inhibitors

All inhibitors of gibberellin used in this study affect synthesis of gibberellin in plants (Fig. 1). Generally, the inhibitors blocked *P. falciparum* growth *in vitro* (Table 1, Fig. S1); although, results were admittedly different among the inhibitors as well as between *Plasmodium* and *Toxoplasma*. For example, inabenfide (INA) exerted strong activities in both *P. falciparum* and *T. gondii*, whereas prohexadione exhibited no cytotoxicity to *P. falciparum* even at 500 µM. Likewise, ED_{50}s of some inhibitors varied greatly between *P. falciparum* and *T. gondii*, such as AMO-1618: 10.3±2.22 µM in *P. falciparum* and >1000 µM in *T. gondii*. Apparent difference in effective inhibitor concentrations between the two parasite species could be species-specific barrier on membranes for drug uptake or inhibitory mechanisms in *P. falciparum* and *T. gondii* [14].

Some of the tested inhibitors have an asymmetric carbon, and their enantiomers are known to differ significantly in their biological properties [15]. (*S*)-forms are biologically more active than (*R*)-forms in higher plants [16]. In order to examine the chirality effect of these inhibitors, we separated enantiomers from commercially available INA by HPLC using a chiral column (Fig. S2) since marketed INA is racemic. The (*S*)-form was slightly more potent than the (*R*)-form, as demonstrated by ED_{50} values of 2.78±0.51 µM and 6.32±0.81 µM, respectively in *P. falciparum* (Table 1). Notably, the (*R*)-form was more effective in inhibiting growth of *T. gondii*.

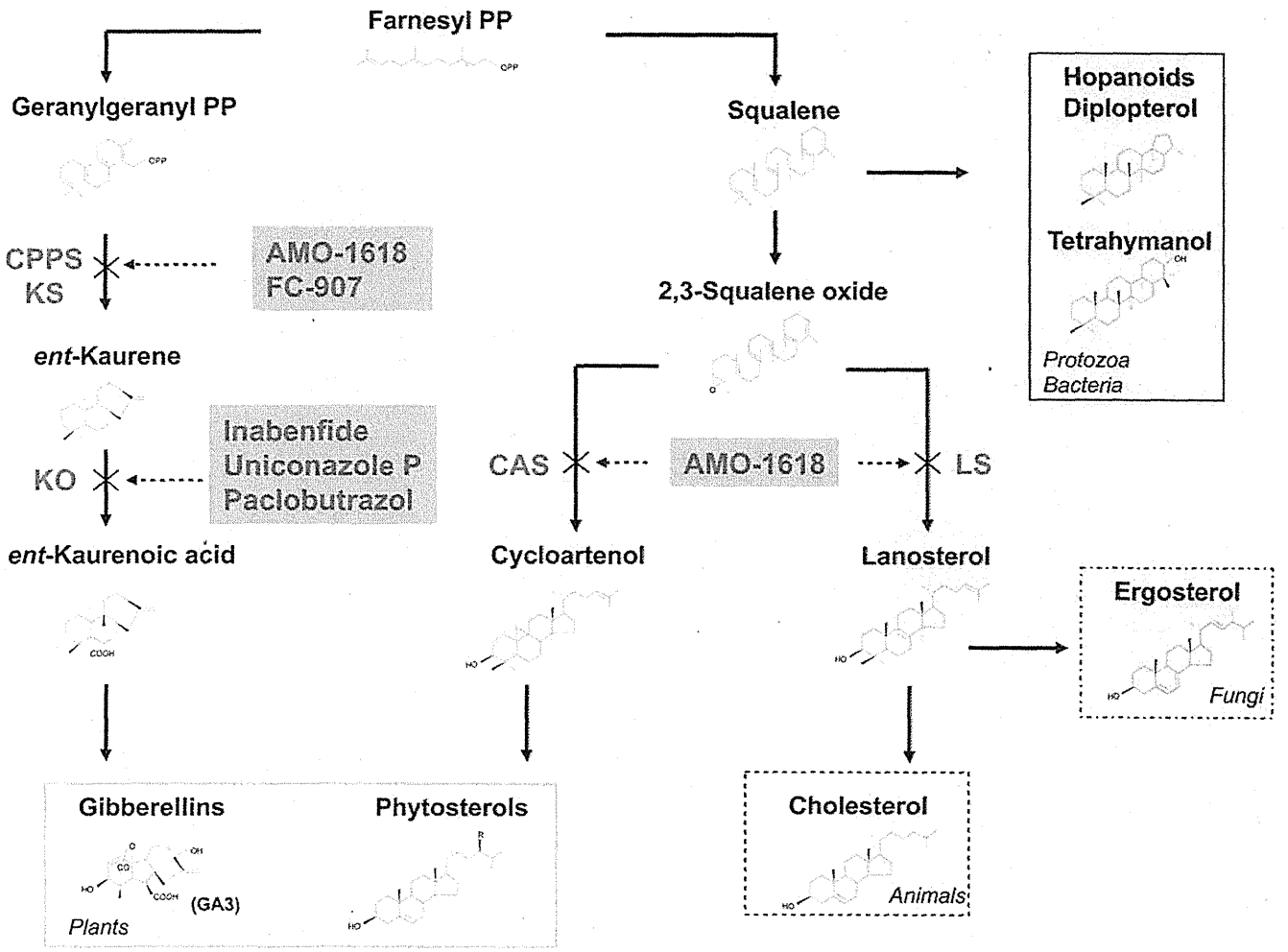

Figure 1. Isoprenoid biosynthetic pathways and known inhibitors in various organisms. Broken arrows indicate blocks in the biosynthesis due to specific inhibitors. "R" indicates various functional groups specific to individual compounds. CPPS, copalyl-diphosphate synthase (EC 5.5.1.13); KO, *ent*-kaurene oxidase (EC 1.14.13.78); CAS, cycloartenol synthase (EC 5.4.99.8); LS, lanosterol synthase (EC 5.4.99.7); KS, *ent*-kaurene synthase (EC 4.2.3.19); PP, pyrophosphate.
doi:10.1371/journal.pone.0032246.g001

Table 1. ED_{50} of the gibberellin biosynthetic inhibitors.

Reagents	ED_{50} of *P. falciparum* (μM)	ED_{50} of *T. gondii* (μM)
Chlorocholine Chloride	8.94±26.08	>10000
AMO-1618	10.3±2.22	>1000
FC-907	4.26±0.14	2206.7±2.46
Inabenfide	2.94±0.15	17.0±1.32
Paclobutrazol	27.1±2.69	120.6±5.38
Uniconazole P	30.7±6.20	97.4±8.66
Ancymidol	322.9±13.1	>1000
Prohexadione	>500	>10000
(*S*)-Inabenfide	2.78±0.51	24.04±1.07
(*R*)-Inabenfide	6.32±0.81	6.23±1.65

Growth inhibitory effects of gibberellin biosynthetic inhibitors and enantiomers of INA to *P. falciparum* and *T. gondii* are shown. Values are the mean ± standard deviations (SD) from three independent experiments, with each treatment duplicated twice. N.D.; not determined.
doi:10.1371/journal.pone.0032246.t001

Morphological changes induced by gibberellin biosynthetic inhibitors

We also evaluated morphological and physiological effects induced by the gibberellin biosynthetic inhibitors. In what appears to be the center of the parasite, a Giemsa-unstained region was prominent within 4 h after treatment with INA (Fig. 2 B). The "haloed" parasites swelled and ruptured within 12 h of culture in immature trophozoite-stage. Rings were seldom found when early trophozoite-stage parasites were treated with INA. When INA was applied at late stages of the parasite, *i.e.* in mature trophozoites and schizonts, a similar swelling was also observed although the stained periphery appears broader with merozoites bloated in appearance and few in number (Fig. 2 C, D). Ring-stage treated parasite cultures were usually appliqué forms (rings appearing on the periphery of the erythrocytes) (Fig. 2 A).

Another type of gibberellin biosynthetic inhibitors, AMO-1618 and FC-907, which prevent cyclization reaction in the early steps of gibberellin biosynthesis (Fig. 1) [15], [17], also caused parasite cells to swell. Swelled parasites were found within 8 h and 24 h after AMO-1618 treatment (Fig. 2, S3), but the altered morphology on schizonts was different: parasites appear abnormally disordered inside erythrocytes (Fig. 2 C, D). A similar morphological change in *Plasmodium* cultures were observed when greater than 2 μM INA were used (data not shown). Notably, both INA and AMO-1618 did not appear to damage erythrocytes, because *P. falciparum* could infect erythrocytes that had been treated for 24 h with 50 μM INA or 250 μM AMO-1618 without any significant inhibitory effects (Fig. S4).

At 2 μM, INA-induced morphological changes were microscopically visible at 24 h in asynchronous parasite cultures. In order to determine if INA and AMO-1618 targets a specific stage during intraerythrocytic development, we increased concentrations of INA to 50 μM and AMO-1618 to 250 μM. Both inhibitors at these concentrations provoked morphological changes more rapidly than concentrations at their ED_{50}s (Fig. S5). The use of increased concentrations of inhibitors also allowed us to measure the intrinsic sensitivity of the parasites *in vitro*, and provided clues to the maximal response that can be produced by these inhibitors, as well as their toxicity to the human erythrocytes. Even after 24 h incubation, use of 0.1% DMSO alone gave no effects on growth and morphology of malaria parasites. Parasite swelling and rupture was also observed on *P. falciparum* cultures treated with other gibberellin biosynthetic inhibitors, such as paclobutrazol and uniconazole P (Fig. S5). These inhibitors, as well as INA, are known to block cytochrome P450-dependent monooxygenases (CYP701A) in plants [15]. Interestingly, the time and the concentrations necessary to provoke morphological changes were different among these compounds, presumably due to differences in solubility and lipophilicity.

The 'haloed' trophozoites

The "haloed" parasites were stained with various fluorescent probes to visualize intracellular components. The center of the trophozoites was not stained with acridine orange (Fig. 3 A). Both nuclei and cytoplasm appear to be on the periphery, as seen in the Giemsa-stained images. Nile Red, used to visualize various lipid-rich compartments such as membranes, endoplasmic reticulum (ER) and lipid bodies [18], revealed a simpler staining pattern surrounding what appears to be fewer merozoites in contrast to the control. Merozoites also appear bloated with intense spots of fluorescence (presumed as lipid bodies, Fig. 3 B). In normal mature stage trophozoites, rhodamine 123 showed thread-like branched mitochondria, characteristic of the mitochondrial development at the later stages where each daughter merozoite receives a branch of the parent organelle (Fig. 3 C) [19]. In INA-treated parasites, however, branched mitochondria were rarely seen. Although fluorescence intensity in the mitochondria started to decrease after 2 h, parasites still have significant fluorescence over the entire parasite cytosol, except in the food vacuole, similar to untreated parasite cells. This observation suggest a membrane potential generated by the parasite's outer plasma membrane [20], [21] and that INA effect likely induced a specific reduction in the mitochondrial membrane potential alone.

These differences in the staining patterns were not evident when ring-stage parasites were observed (data not shown), which suggest that various membranes were remarkably affected by INA only when parasites reached the trophozoite stage. The timing is coincident at a time when the parasite starts to actively generate membranes needed for growth and schizogony [22].

Electron microscopy also revealed fine intracellular differences at the trophozoite and schizont-stage parasite (Fig. 4 A, B). When trophozoites were treated with INA or AMO-1618 (Fig. 4 A), membranes of the nuclear envelope and ER were thicker and intensely stained compared to control parasites. Conspicuously unfamiliar spaces appeared around the ER and daughter nuclei (Fig. 4 A, INA and AMO-1618 panel). Using asynchronous cultures, these spaces were more readily observed at mature-stage parasites than early trophozoites (Fig. 4 B, b and f vs. c and d). No differences were evident in the plasma membranes of both host and parasite cells during the intraerythrocytic life cycle (Fig. 4 B). These results suggest that the gibberellin biosynthetic inhibitors appear to affect components of various intracellular membranes of the parasites, and the effects were especially evident during schizogony.

INA effect and osmotic pressure in parasite cells

Various stressful conditions were applied to INA treated parasite: use of hydraulic pressure, ultrasound, pH (5–9) and temperature changes (4–37°C); but no differences were observed when compared to control parasites (DMSO-treated). However, different responses were seen when trophozoite-stage parasites were under various osmotic stress. Hyperosmotic conditions were achieved by incubating with 10% (v/v) 1×, 2×, 3× or 4× PBS. For control, untreated parasite cultures, relative parasitemia drastically decreased with increasing hyperosmotic environment (Fig. 5 A). However, relative parasitemia in the INA-treated

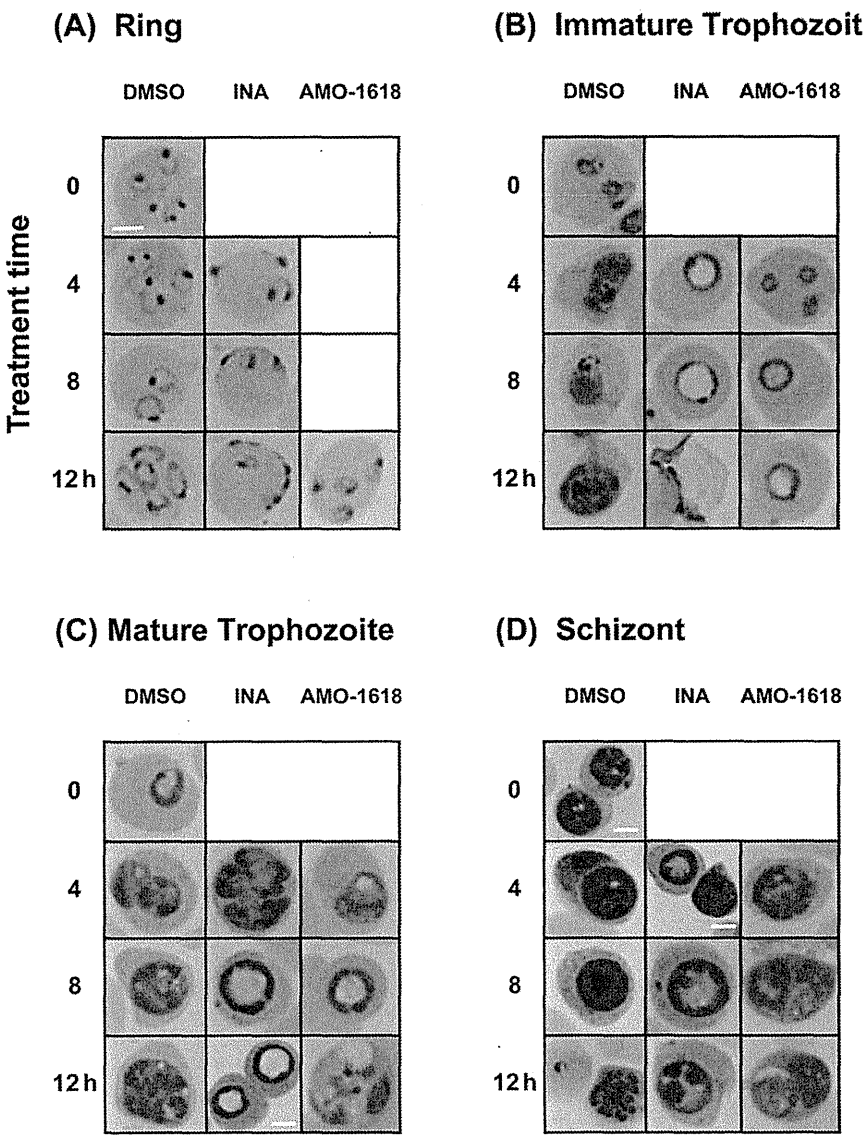

Figure 2. Effect of INA and AMO-1618 on intraerythrocytic development of *P. falciparum*. Tightly synchronized parasite cells that have undergone 5% sorbitol treatment and percoll density gradient centrifugation (window period: 4 h) were treated with 1 μl/ml DMSO, 50 μM INA or 250 μM AMO-1618 at different parasite stages: after 0 h (ring, A), 20 h (immature trophozoite, B), 28 h (mature trophozoite, C) and 36 h (schizont, D). Cultures were examined after 4, 8 and 12 h using Giemsa thin blood smears. Scale bar: 3 μm; all images without a scale bar are displayed at the same scale as the left uppermost image in (A).
doi:10.1371/journal.pone.0032246.g002

samples increased in higher hyperosmotic environment, especially in cultures treated with 10% 4× PBS. Moreover, 'haloed' trophozoites were less evident in cultures incubated with 3× or 4× PBS. To examine the potential effects of cation species, we made a solution where the net solute was the same to PBS but the concentrations of Na^+ and K^+ were reversed (137 mM KCl, 8.1 mM K_2HPO_4, 2.68 mM NaCl, and 1.47 mM NaH_2PO_4). Between normal and reversed PBS in the different treatments, no significant differences were observed in both parasitemia and morphology (Fig. S6). Exogenously added Ca^{2+} (100 μM) to cultures did not help reverse the 'haloed' effects of INA in trophozoites (Fig. S7).

Hyposmotic stress enhanced INA's effect in treated parasites: early trophozoite-stage parasites swelled even more by the addition of 10% (v/v) water to the culture medium (Fig. 5 B). At 40% (v/v) water, trophozoites swelled to almost the same volume of the infected erythrocyte. Decrease in parasitemia was also statistically significant compared to the control. These observations suggest that INA treatment might affect membrane permeability; water or ion influx might cause swelling of the parasites.

Isoprenoid biosynthetic pathway in apicomplexan parasites

Parasite cultures were incubated with gibberellin A_3 and A_4, the most effective gibberellins, with or without gibberellin biosynthetic inhibitors. Of note, gibberellins did not affect growth of parasites nor overcome the effects of the inhibitors (data not shown), suggesting that the inhibitors could not disrupt gibberellin biosynthesis in *P. falciparum* or malaria parasites do not utilize gibberellins.

Gibberellins are diterpene (isoprenoid), ubiquitous and essential compounds by themselves or as materials of secondary metabolites

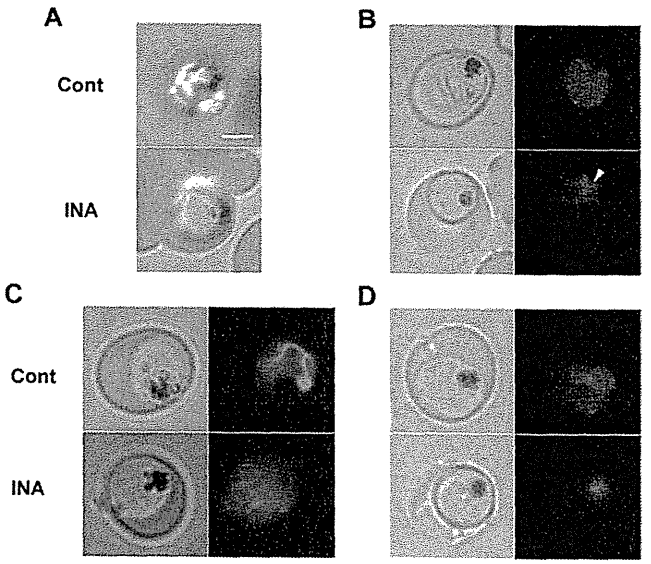

Figure 3. Fluorescence microscopy of INA-treated parasites. Infected erythrocytes were stained with (A) acridine orange, (B) Nile Red, (C) rhodamine 123 and (D) LysoTracker™ Red DND-99. INA was introduced at: (A) 100 μM for 9 h, (B) 50 μM for 6 h, and (C and D) 50 μM for 4 h. 100 μg/ml acridine orange was applied to thin blood smears made from intraerythrocytic parasites treated with INA. For other fluorescence dyes, *P. falciparum* cultures were incubated with probes for 1 h at the following concentrations: Nile Red, 1 μg/ml; rhodamine 123, 10 ng/ml; and LysoTracker® Red DND-99, 75 nM. Cells were not washed prior to fluorescence microscopy to minimize damage due to osmotic changes. Scale bar, 3 μm. An arrow indicates a lipid body in (B).
doi:10.1371/journal.pone.0032246.g003

and signal molecules in animals, plant and bacteria [15]. Biosynthetic pathways of isoprenoids are very complicated and parallel pathways for the biosynthesis of the universal 5-carbon building block for all terpenoid compounds exist. A huge variety of sterols and terpenoids are synthesized via isoprenoid metabolic pathways in a species-specific manner, although all pathways utilize farnesyl pyrophosphate as a starting molecule generated in the mevalonate pathway and the 2-*C*-methyl-D-erythritol 4-phosphate (MEP) pathway (Fig. 1) [23]. Gibberellin biosynthetic inhibitors have been known to block other enzymes leading to the production of sterols and terpenoids. We then analyzed *P. falciparum* treated with INA and AMO-1618 by GC-MS. Interestingly, any sterols or terpenoids besides cholesterol derived from human erythrocytes were not detected, and there were no significant differences in the level of cholesterol between control and INA- or AMO-1618-treated samples (Fig. 6).

Discussion

Efforts on malaria control have been complicated by emergence of drug resistance. With the apicoplast considered to originate from an ancestor with an endosymbiotic alga, and that many non-photosynthetic processes are shared peculiarly with plants, plant growth regulators are of particular interest for pharmaceutical leads on the assumption that the molecular target may not be present in humans. The present study clearly showed some inhibitors that antagonize gibberellin biosynthesis in plants are effective to both *P. falciparum* and *T. gondii* (Table 1). Gibberellin is one of 5 major plant hormones known to exert various effects on physiological events, particularly germination and seed bearing by promoting cell elongation [24]. 126 different gibberellins are known to occur in plants [15], and they are synthesized via the mevalonate pathway and the MEP pathway. Interestingly, gibberellin has been utilized to induce development of parthenocarpous fruits in some fruits such as grapes. On the other hand, gibberellin inhibitors have also been widely used for agriculture, *e.g.* for dwarf plants without harmful effects to either plants or animals.

All gibberellin inhibitors tested in this study block biosynthesis of gibberellin in plants: AMO-1618 and FC-907 block synthesis of *ent*-kaurene (an intermediate during the synthesis of gibberellin) by inhibition of copalyl-diphosphate synthase (CPPS) and *ent*-kaurene synthase (KS, Fig. 1) [15]. Next to AMO-1618 and FC-907 steps, INA, paclobutrazol, uniconazole P and ancymidol interrupt *ent*-kaurene oxidase (KO), a member of the cytochrome P450 monooxygenases (CYP) oxidating *ent*-kaurene into *ent*-kaurenoic acid. Azole antifungal such as fluconazole and diniconazole are analogous compounds to these inhibitors and interrupt synthesis of ergosterol [25]. They have an asymmetric carbon and their enantiomers are known to differ significantly in their biological properties [16], [26]. (*R*)-forms demonstrate stronger activity than (*S*)-forms in terms of fungicidal effects, whereas the latter is functionally active and the (*R*)-forms showed only residual activity with regard to blockage in plant gibberellin biosynthesis. We tested the stereochemical selectivity of INA and found that the (*S*)-form inhibited growth of *P. falciparum* >2 times stronger than (*R*)-form but *vice versa* in *T. gondii* (Table 1). The stereochemical discrimination was, thus, similar to plants than to fungi in *P. falciparum*, although the (*S*)-form was reportedly 1000 times more potent than (*R*)-form in growth retardation of pumpkin seedlings [26]. Differences may be due to discrepancies in protein structures that relate to membrane permeability or translocation of the enantiomers to the site of biosynthesis in such distant species.

The observed decrease in parasitemia in INA-treated cultures correlated with remarkable morphological changes: swelling and rupture of *P. falciparum* cells, particularly when drug treatment commenced during early trophozoite stage (Fig. 2). Trophozoite-stage parasite cells appear to be 'haloed', the center of the cell remains unstained by Giemsa and acridine orange. Both nuclei and cytoplasm were seen on the periphery of the parasite cells. These data suggest that some substances that are neither acidic nor alkaline might accumulate in the unstained parts.

We also observed the intracellular structures in INA-treated cultures using different dyes and found that various intracellular organelles, especially organelles synthesized during schizogony (such as mitochondria, membrane network and food vacuoles) are morphologically abnormal or compromised after short treatment with INA (Fig. 3). Membrane potential in the mitochondria was reduced rapidly within 2 h of INA treatment. Organelle membranes such as those in the ER and nuclear envelope appeared thicker and gaps were observed around such organelles under electron microscopy (Fig. 4). From these observations, it appears that gibberellin biosynthetic inhibitors damage the parasite internal organelles, compromises parasite membranes and results to abnormalities in the treated parasites.

In order to further probe for clues that can shed light into the mechanisms for such changes in the membranes, we exposed INA-treated parasite cells to various stresses, and found that osmotic pressure modified the effects of INA. Treated parasite cells under hyperosmotic conditions became less swelled and viability was significantly restored (Fig. 5 A). In contrast, the addition of water in the culture medium enhanced expansion and rupture of parasites (Fig. 5 B). These results demonstrate that INA treatment might affect permeability of membranes, and consequently result to uncontrollable influx of water or ion into parasite cells. No abnormalities in the plasma membrane structure were observed by electron microscopy (Fig. 4), although this cannot be completely ruled out since parasites with severely compromised plasma

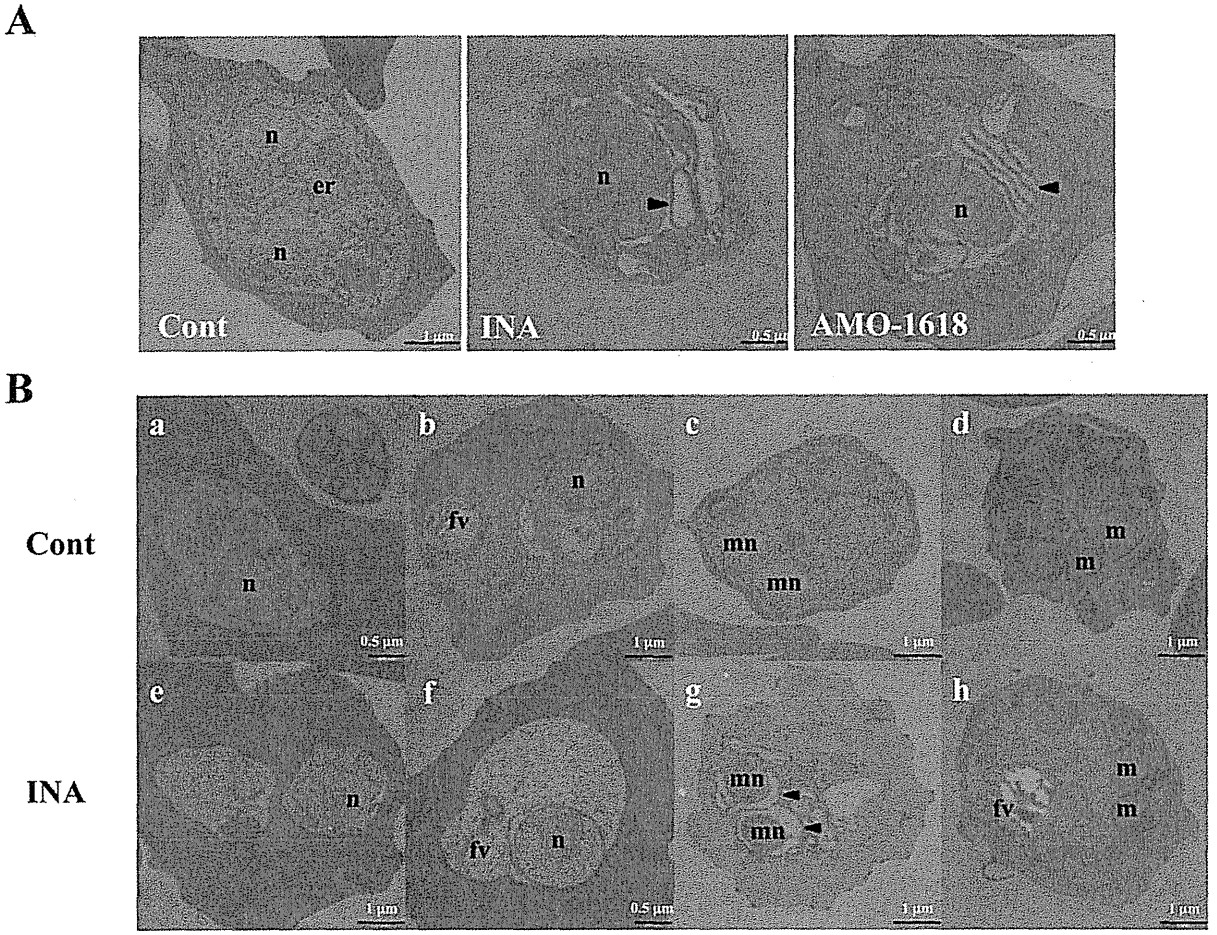

Figure 4. Transmission electron microscopy of parasitized erythrocytes treated with inhibitors. (A) Sections through an erythrocyte containing a trophozoite-stage parasite exposed to 0.1% DMSO for 6 h, 50 μM INA for 6 h or 250 μM AMO-1618 for 8 h, respectively. (B) Asynchronized parasites were treated with 0.1% DMSO (a–d) or 50 μM INA for 6 h (e–h). Sections from representative stages during intraerythrocytic development: ring- (a and e), early trophozoite- (b and f), mature trophozoite- (c and g) and schizont-stage parasites (d and h) are shown. Nuclei (n), food vacuoles (fv), merozoites (m), nuclei of merozoites (mn) and abnormal gaps between the nuclei and the nuclear envelopes (arrowheads) are indicated. Scale bar is indicated at the bottom of the images.
doi:10.1371/journal.pone.0032246.g004

membranes are very likely susceptible to rupture or bursting during various treatments for microscopy.

In order to maintain the various functions and stability of plasma membranes, different organisms synthesize several specific components for their biological membranes. For example, sterols, a vast family of isoprenoids, take pivotal role with mammalian and fungal cells generally synthesizing one major sterol, cholesterol and ergosterol, respectively [23], [27]. Plants, on the other hand, are known to produce a characteristically complex sterol mixture. As many as 61 sterols and isoprenoids have been identified in a single maize seedling [28]. Prokaryotes produce hopanoids, pentacyclic isoprenoids, by direct cyclization of squalene (Fig. 1) [29]. The functions of the hopanoids were shown to be equivalent to sterols: functioning as membrane reinforcers affecting membrane permeability and fluidity. In protozoa, there has been one report that *Tetrahymena* synthesizes tetrahymanol, a quasi-hopanoid, together with small amounts of diplopterol [30], [31]. Both components were incorporated into its membranes.

Enzymes that are involved in gibberellin biosynthesis are also of importance in the formation of such sterols and other membrane constituents. Change in the level of these substances after treatment with inhibitors has been often observed as side activities for these inhibitors [15]. For example, AMO-1618 inhibits syntheses of phytosterols and cholesterol, by blocking cycloartenol synthase (CAS) in plants and lanosterol synthase (LS) in animals, respectively [32].

We analyzed *P. falciparum* treated with INA and AMO-1618 by GC-MS in order to identify sterols or isoprenoids in malaria parasites, but we could not detect any isoprenoids, besides cholesterol (Fig. 6). We might be able to hypothesize that responsible components could be too low or structurally unknown to detect by GC-MS in parasite cells. Data about syntheses of isoprenoids in protozoa, especially in *Apicomplexa*, remains nil. Intraerythrocytic parasites are known to intake large amounts of erythrocyte contents with surrounding membranes that are cholesterol rich, however, cholesterol is greatly depleted in parasite membranes (Fig. 6 A) [33]. How parasites transport and dispose of excess cholesterol within the cells remain a puzzle. Additionally, does lack of isoprenoids make membranes leaky even in intracellular parasites? A previous study has demonstrated by differential scanning calorimetry and electron spin resonance the association of gibberellin molecules with phospholipid membranes thereby altering the fluidity or viscosity of the lipid bilayer [34]. Clearly, further studies on gibberellin biosynthetic inhibitors could shed light if these compounds could perturb lipid bilayers or alter properties of the membrane phospholipid.

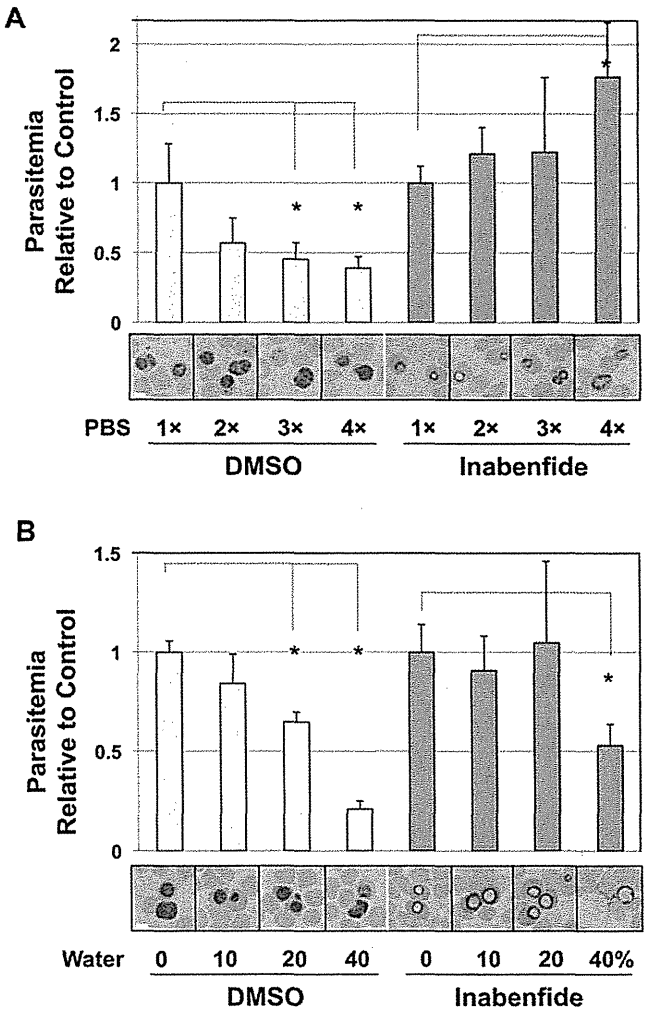

Figure 5. Effects of osmotic pressure to intraerythrocytic parasites treated with INA. (A) Effects of hyperosmotic stress in INA-treated parasites. *P. falciparum* cultures treated with 50 μM INA were observed in various dilution ratios of PBS for 8 h. Parasitemia was determined by Giemsa-stained thin blood smears. Student's *t*-test: *P>0.005. Values are means ± SD of n=6 in two independent experiments. Data were normalized relative to control cultures (1 × PBS) in DMSO- and INA-treated samples, respectively. Representative parasite morphologies are shown for each treatment. Scale bar, 3 μm. (B) Effects of hyposmotic stress, experimentally induced by the addition of water to the culture medium of *P. falciparum*, after 8 h of 50 μM INA treatment. N=6 smears each in two independent experiments.
doi:10.1371/journal.pone.0032246.g005

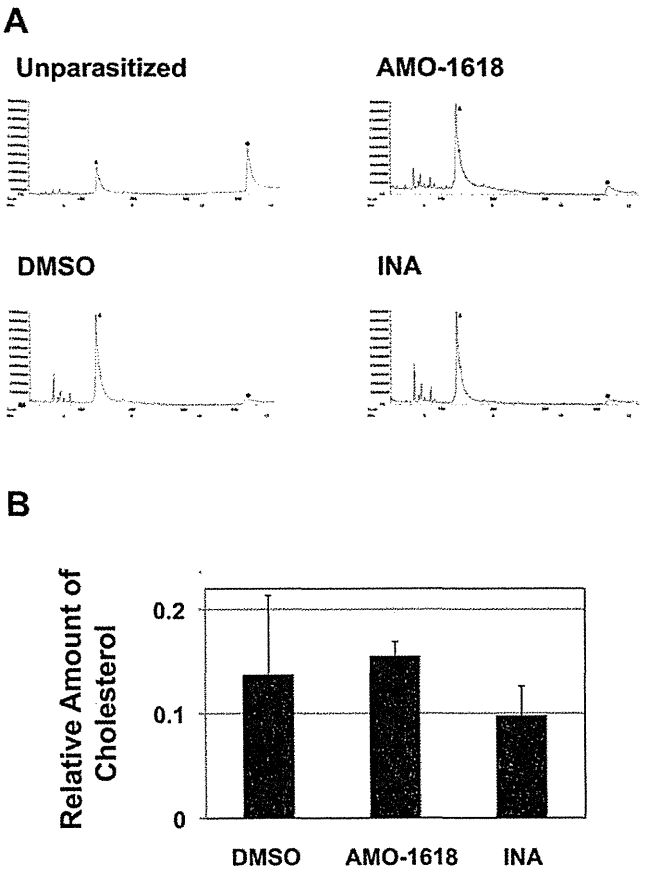

Figure 6. GC-MS analysis of isoprenoids in *P. falciparum in vitro* cultures. (A) Total ion chromatograms of extracts from unparasitized erythrocytes (Unparasitized), parasites treated with 0.1% DMSO, 250 μM AMO-1618, and 50 μM INA for 6 h. Triangles and circles indicate the peaks of geranylgeraniol mixed as an internal control (retention time=6.57 min) and cholesterol (11.23 min), respectively. These compounds were identified by direct comparison with authentic samples. (B) Quantification of cholesterol in each treated sample. Cholesterol amount was calculated from the peak areas and normalized relative to the ratio of the internal control geranylgeraniol. Values are means and SD of triplicate measurements of a representative experiment.
doi:10.1371/journal.pone.0032246.g006

The gibberellin biosynthetic inhibitors are known to be specific for isoprenoid biosynthesis in plants. We searched amino acid sequences and conserved domain sequences essential for these enzymes using PlasmoDB, but no sequences with significant homologies were found. This may imply the uniqueness of isoprenoid metabolic pathways in *Apicomplexa*, and consequently, provide potent targets to develop novel therapeutic agents.

Supporting Information

Figure S1 Concentration-response curve of INA. Each point represents the mean ± standard deviations (SD) from three independent experiments, with each treatment duplicated twice. (TIF)

Figure S2 Chiral separation of enantiomeric INA. Racemic form of INA was separated on Chiralcel OD column. Mobile phase: n-hexane-2-propanol (8:2, v/v), flow rate:10 ml/min, detection: 275 nm. HPLC chromatograms of each enantiomer are also shown.
(TIF)

Figure S3 Effect of gibberellin biosynthetic inhibitors on the intraerythrocytic development of *P. falciparum*. Asynchronized parasites were treated with 200 μM FC-907 for 24 h, 500 μM uniconazole P for 8 h, 200 μM paclobutrazol for 8 h, 50 μM INA or 1 μl/ml DMSO for 6 h. Giemsa-stained thin blood smears were prepared from each sample after the indicated treatment and examined under a microscope. Each panel shows the typical morphology of trophozoite-stage parasites in each treatment. Scale bar, 3 μm.
(TIF)

Figure S4 Effects of gibberellin biosynthetic inhibitors on the viability of erythrocytes to support growth of *P. falciparum*. Erythrocytes that had been incubated in RPMI

1640 containing 10% human serum and supplemented with 1 μl/ml DMSO, 50 μM INA or 250 μM AMO-1618 for 24 h were washed with RPMI 1640 twice and mixed with *P. falciparum* infected erythrocytes at 0.3% starting parasitemia. Thin blood films from each culture were prepared after 48 h, stained with Giemsa and parasitemias were counted under a microscope. Values are mean ± SD of n = 3 in each representative experiment.
(TIF)

Figure S5 Influence of INA concentration on growth inhibition in *P. falciparum*. (A) Synchronized parasites at early trophozoite stage were treated with 0 (1 μl/ml DMSO), 10 or 50 μM INA for 0–8 h. Parasitemia was determined by thin blood films after staining with Giemsa. Error bars represent the standard deviation (SD) of three independent experiments made in duplicate. Data are normalized relative to those for the control treated for 0 h. (B) The parasites treated with 0, 10 or 50 μM INA after 4 h, stained with Giemsa, and visualized under light microscope. Scale bar = 3 μm. Each panel shows the typical morphology of trophozoite-stage parasites in each treatment.
(TIF)

Figure S6 Effects of cation species to the parasitemia of the intraerythrocytic parasites treated with INA. Synchronized parasites at early trophozoite stage were mixed with 10% of 1× and 4× normal PBS or the solution that Na^+ and K^+ concentrations in PBS are exchanged (reversed-PBS; 1× reversed-PBS contains 137 mM KCl, 8.1 mM K_2HPO_4, 2.68 mM NaCl, 1.47 mM NaH_2PO_4), and treated with 50 μM INA or 1 μl/ml DMSO for 8 h. Parasitemia was determined by counting thin blood film from each culture blindly after staining with Giemsa; the counter was blinded to sample identities. Error bars represent the standard deviation of three independent experiments made in duplicate. Data are normalized relative to those for the control treated with 1× PBS and 1 μl/ml DMSO.
(TIF)

Figure S7 Influence of Ca^{2+} on the effects of INA in *P. falciparum*. Parasites were synchronized by 5% sorbitol treatment and treated with 1 μl/ml DMSO or 50 μM INA with or without adding 100 μM $CaCl_2$ after 18 h of incubation. The parasites were examined at 6 h of the treatment by thin blood smears and staining with Giemsa. Scale bar indicates 3 μm. Each panel shows a typical morphology of trophozoite-stage parasites in each treatment.
(TIF)

Acknowledgments

The authors greatly appreciate Prof. Yuji Kamiya (RIKEN, Japan) for kindly providing FC-907. We are deeply grateful to Dr. Eri Hayakawa (Tokyo Women's Medical University, Japan) for technical advice, Hiroko Omori (Osaka University, Japan) for expert work in transmission electron microscopy, Yohei Ueno (Graduate school of agriculture, TUAT, Japan) for GC-MS, and Sawako Itagaki and Mayumi Fukui (Osaka University, Japan) for culturing and counting parasitemia.

Author Contributions

Conceived and designed the experiments: TT KN NMQP HK TH KT. Performed the experiments: TT MT KN HK. Analyzed the data: TT MT KN HK. Contributed reagents/materials/analysis tools: KA YH. Wrote the paper: TT KN KA NMQP HK KT.

References

1. Eastman RT, Fidock DA (2009) Artemisinin-based combination therapies: a vital tool in efforts to eliminate malaria. Nat Rev Microbiol 7: 864–874.
2. Adeyi O, Atun R (2010) Universal access to malaria medicines: innovation in financing and delivery. Lancet 376: 1869–1871.
3. Noedl H, Se Y, Schaecher K, Smith BL, Socheat D, et al. (2008) Evidence of artemisinin-resistant malaria in Western Cambodia. N Engl J Med 361: 2619–2620.
4. Miranda K, Pace DA, Cintron R, Rodrigues JCF, Fang J, et al. (2010) Characterization of a novel organelle in *Toxoplasma gondii* with similar composition and function to the plant vacuole. Mol Microbiol 76: 1358–1375.
5. Wiesner J, Borrmann S, Jomaa H (2003) Fosmidomycin for the treatment of malaria. Parasitol Res 90: S71–S76.
6. Fichera ME, Roos DS (1997) A plastid organelle as a drug target in apicomplexan parasites. Nature 390: 407–409.
7. Jomaa H, Wiesner J, Sanderbrand S, Altincicek B, Weidemeyer C, et al. (1999) Inhibitors of the nonmevalonate pathway of isoprenoid biosynthesis as antimalarial drugs. Science 285: 1573–1576.
8. Nagamune K, Hicks LM, Fux B, Brossier F, Chini EN, et al. (2008) Abscisic acid controls calcium-dependent egress and development in *Toxoplasma gondii*. Nature 451: 207–210.
9. Kato M, Sasahara K, Ochi K, Akita H, Oishi T (1991) Asymmetric reduction of 2-aminobenzophenone using yeast, *Rhodosporidium toruloides*. Chem Pharm Bull 39: 2498–2501.
10. Trager W, Jensen JB (1976) Human malaria parasites in continuous culture. Science 193: 673–675.
11. Dobrowolski JM, Sibley LD (1996) Toxoplasma invasion of mammalian cells is powered by the actin cytoskeleton of the parasite. Cell 84: 933–939.
12. McFadden DC, Seeber F, Boothroyd JC (1997) Use of *Toxoplasma gondii* expressing beta-galactosidase for colorimetric assessment of drug activity *in vitro*. Antimicrob Agents Chemother 41: 1849–1853.
13. Yuan LC, Gulyas BJ (1981) An improved method for processing single cells for electron microscopy utilizing agarose. Anat Rec 201: 273–281.
14. Nair SC, Brooks CF, Goodman CD, Strurm A, McFadden GI, et al. (2011) Apicoplast isoprenoid precursor synthesis and the molecular basis of fosmidomycin resistance in *Toxoplasma gondii*. J Exp Med 208: 1547–1559.
15. Rademacher W (2000) Growth retardants: effects on gibberellin biosynthesis and other metabolic pathways. Annu Rev Plant Physiol Plant Mol Biol 51: 501–531.
16. Furuta R, Doi T (1994) Chiral separation of diniconazole, uniconazole and structurally related compounds by cyclodexrin-modified micellar electrokinetic chromatography. Electrophoresis 15: 1322–1325.
17. Hedden P, Phinney BO, MacMillan J, Sponsel VM (1977) Metabolism of kaurenoids by *Gibberella fujikuroi* in the presence of the plant growth retardant, N, N, N-trimethyl-1-methyl-(2′,6′,6′-trimethylcyclohex-2′-en-1′-yl) prop-2-enylammonium iodide. Phytochemistry 16: 1913–1917.
18. Palacpac NM, Hiramine H, Seto S, Hiramatsu R, Horii T, et al. (2004) Evidence that *Plasmodium falciparum* diacylglycerol acyltransferase is essential for intraerythrocytic proliferation. Biochem Biophys Res Commun 321: 1062–1068.
19. van Dooren GG, Marti M, Tonkin CJ, Stimmler LM, Cowman AF, et al. (2005) Development of the endoplasmic reticulum, mitochondrion and apicoplast during the asexual life cycle of *Plasmodium falciparum*. Mol Microbiol 57: 405–419.
20. Tanabe K (1983) Staining of *Plasmodium yoelii*-infected mouse erythrocytes with the fluorescent dye rhodamine 123. J Protozool 30: 707–710.
21. Divo AA, Geary TG, Jensen JB, Ginsburg H (1985) The mitochondrion of *Plasmodium falciparum* visualized by rhodamine 123 fluorescence. J Protozool 32: 442–446.
22. Mamoun BC, Prigge ST, Vial H (2010) Targeting the lipid metabolic pathways for the treatment of malaria. Drug Dev Res 71: 44–55.
23. Hartman M-A (1998) Plant sterols and the membrane environment. Trends Plant Sci 3: 170–175.
24. Hedden P, Kamiya Y (1997) Gibberellin biosynthesis: enzymes, genes and their regulation. Annu Rev Plant Physiol Plant Mol Biol 48: 431–460.
25. Yoshida Y (1988) Cytochrome P450 of fungi: primary target for azole antifungal agents. Curr Top Med Mycol 2: 388–418.
26. Miki T, Kamiya Y, Fukuzawa M, Ichikawa T, Sakurai A (1990) Sites of inhibition by a plant-growth regulator, 4′-chloro-2′-(alpha-hydroxybenzyl)-isonicotinanilide (inabenfide), and its related compounds in the biosynthesis of gibberellins. Plant Cell Physiol 31: 201–206.
27. Haines TH (2001) Do sterols reduce proton and sodium leaks through lipid bilayers? Prog Lipid Res 40: 299–324.
28. Guo DM, Venkatramesh M, Nes WD (1995) Developmental regulation of sterol biosynthesis in *Zea mays*. Lipids 30: 203–219.
29. Kaneda T (1991) Iso- and anteiso-fatty acids in bacteria: biosynthesis, function, and taxonomic significance. Microbiol Rev 55: 288–302.

30. Saar J, Kader J-C, Poralla K, Ourisson G (1991) Purification and some properties of the squalene-tetrahymanol cyclase from *Tetrahymena thermophila*. Biochim Biophysic Acta 1075: 93–101.
31. Welander PV, Hunter RC, Zhang L, Sessions AL, Summons RE, et al. (2009) Hopanoids play a role in membrane integrity and pH homeostasis in *Rhodopseudomonas palustris* TIE-1. J Bacteriol 191: 6145–6156.
32. Seo S, Tonda K, Uomori A, Takeda K, Hirata M (1993) Effect of sterol biosynthesis inhibitors, SSF-109, on cholesterol synthesis in isolated rat hepatocytes. Steroids 58: 74–78.
33. Jackson KE, Knonis N, Ferguson DJP, Adisa A, Dogovski C, et al. (2004) Food vacuole-associated lipid bodies and heterogeneous lipid environments in the malaria parasite, *Plasmodium falciparum*. Mol Microbiol 54: 109–122.
34. Pauls KP, Chambers JA, Dunbrofe EB, Thompson JE (1982) Perturbation of phospholipid membranes by gibberellins. New Phytol 91: 1–17.

10. Shimizu, M., Satou, K., Nishioka, N., Yoshino, T., Momotani, E. and Ishikawa, Y. 1989. Serological characterization of viruses isolated from experimental mucosal disease. *Vet. Microbiol.* **19** : 13−21.
11. Nagai, M., Sakoda, Y., Mori, M., Hayashi, M., Kida, H. and Akashi, H. 2003. Insertion of cellular sequence and RNA recombination in the structural protein coding region of cytopathogenic bovine viral diarrhoea virus. *J. Gen. Virol.* **84** : 447−452.
12. Kummerer, B. M., Tautz, N., Becher, P., Thiel, H−J. and Meyers, G. 2000. The genetic basis for cytopathogenicity of pestiviruses. *Vet. Microbiol.* **77** : 117−128.
13. Yamane, D., Nagai, M., Ogawa, Y., Tohya, Y. and Akashi, H. 2005. Enhancement of apoptosis via an extrinsic factor, TNF−alpha, in cells infected with cytopathic bovine viral diarrhea virus. *Microbes Infect.* **7** : 1482−1491.
14. Yamane, D., Kato, K., Tohya, Y. and Akashi, H. 2006. The double−stranded RNA−induced apoptosis pathway is involved in the cytopathogenicity of cytopathogenic Bovine viral diarrhea virus. *J. Gen. Virol.* **87** : 2961−2970.
15. Yamane, D., Kato, K., Tohya, Y. and Akashi, H. 2008. The relationship between the viral RNA level and upregulation of innate immunity in spleen of cattle persistently infected with bovine viral diarrhea virus. *Vet. Microbiol.* **129** : 69−79.
16. Yamane, D., Zahoor, M.A., Mohamed, Y.M., Kato, K., Tohya, Y. and Akashi, H. 2009. Microarray analysis reveals distinct signaling pathways transcriptionally activated by infection with bovine viral diarrhea virus in different cell types. *Virus Res.* **142** : 188−199.
17. Yamane, D., Zahoor, M. A., Mohamed, Y. M., Azab, W., Kato, K., Tohya, Y. and Akashi, H. 2009. Inhibition of sphingosine kinase by Bovine viral diarrhea virus NS3 is crucial for efficient viral replication and cytopathogenesis. *J. Biol. Chem.* **284** : 13648−13659.
18. Zahoor, M. A., Yamane, D., Mohamed, Y. M., Kobayashi, K., Kato, K., Tohya, Y. and Akashi, H. 2009. Characterization and application of monoclonal antibodies to bovine viral diarrhea virus nonstructural protein 5A. *Arch. Virol.* **154** : 1745−1754.
19. Zahoor, M. A., Yamane, D., Mohamed, Y. M., Suda, Y., Kobayashi, K., Kato, K., Tohya, Y. and Akashi, H. 2010. Bovine viral diarrhea virus nonstructural protein 5A interacts with NIK and IKKβ−binding protein (NIBP). *J. Gen. Virol.* **91** : 1939−1948.

レビュー

アピコンプレクス門原虫が産生する植物ホルモン様物質とその作用

永宗喜三郎（国立感染症研究所　寄生動物部）

1. アピコンプレクス門原虫の進化学的位置

現在，真核生物は８つのスーパーグループに大別できるという説が広く受け入れられつつある（図１）。その中で哺乳動物や酵母はオピストコンタと呼ばれる単一のグループに分類されており，以前よく言われていた「酵母からヒトまで広く保存されている」というフレーズは，今では真核生物の一つのスーパーグループを代表するという意味でしかなくなりつつある。また，これら８つのスーパーグループの中で，実に７つのスーパーグループにいわゆる「寄生生物」が存在している点は，寄生生物の進化を考

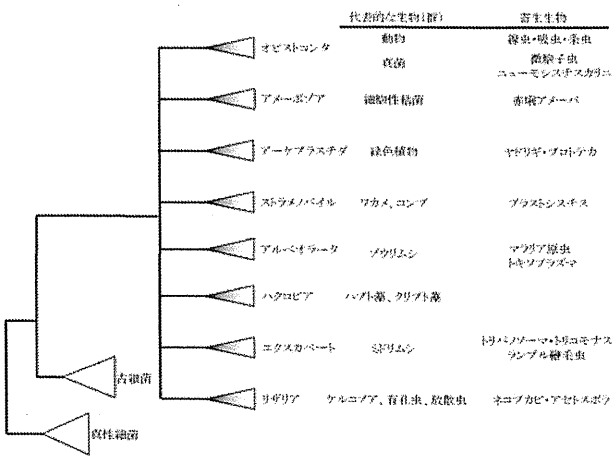

図1 真核生物の8つのスーパーグループ。各グループに属する代表的な生物と寄生生物も示した。

える上で実に興味深い事実である。すなわち，寄生生物は単一の祖先生物から分化したのではなく，様々に進化した生物がそれぞれの事情により「寄生」する道を選択したと考えられる。「寄生」という現象はそれほど魅力的なものなのか，多くの生物を寄生生物への進化に突き動かしている要因は何か，非常に面白く興味をそそるテーマであるが，いまだその答えは得られていない。

さて，これらのスーパーグループの中で，著者が興味を持っている対象であるトキソプラズマやマラリア原虫が属しているアピコンプレクス門は，アルベオラータと呼ばれるスーパーグループに属している。アピコンプレクス門に属する原虫には現在5,000種以上が知られており，全てが寄生性の原生生物である [5]。この中にはマラリア原虫やトキソプラズマ，クリプトスポリジウムなど人類にとって大きな脅威となっている感染症の病原体や，バベシアやアイメリアなど獣医，畜産学領域で大きな問題になっている病原体が含まれている [6, 13]。

それでは次に，現在考えられているアピコンプレクス門原虫の進化の道筋を見てみよう（図2）。現在報告されている中でアピコンプレクス門原虫に最も近縁な生物はクロメラと呼ばれるサンゴに共生している藻類である [7]。クロメラは光合成能を有しているが寄生能力は持っていない。後述する通り，アピコンプレクス門原虫の祖先は光合成をしていたと考えられており，クロメラとアピコンプレクス門原虫の遺伝的近縁性はその傍証の一つとなっている。クロメラの祖先とアピコンプレクス門原虫の祖先が分岐したのは，およそ4億2千万年前のことであり，

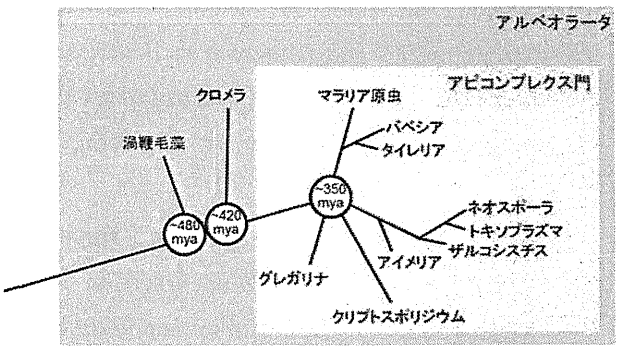

図2 アピコンプレクス門の進化。アピコンプレクス門に属する生物種は今からおよそ3億5千万年前以降にそれぞれ分化したと推定されている（Wellems *et al.* (2009) より改変）[12]。

その後今から約3億5千万年前以降に，現在のアピコンプレクス門原虫の種が分化，成立していったものと考えられている [12]。一方で鳥類の祖先が哺乳動物の祖先と分岐したのが約4億年前のことであると推定されていることと合わせて考えると [9]，アピコンプレクス門原虫間の進化的距離が想像しやすいであろう。

アピコンプレクス門に属する原虫の大きな特徴の一つとして，アピコプラストと呼ばれるオルガネラの存在が挙げられる。アピコプラストは葉緑体が退化してできた4重膜構造の細胞内小器官であり，通常の葉緑体は光合成細菌が植物の祖先に取り込まれて進化したものとされているが，アピコプラストは光合成細菌を取り込んだ紅藻類の祖先が原虫の祖先生物に取り込まれることによって成立したと考えられている [1]（図3）。そのために，アピコプラストは独特の四重膜構造をとる。現在ではアピコプラストは光合成能を失ったものの，脂肪酸合成などの機能を今でも担っており，したがって原虫にとって必

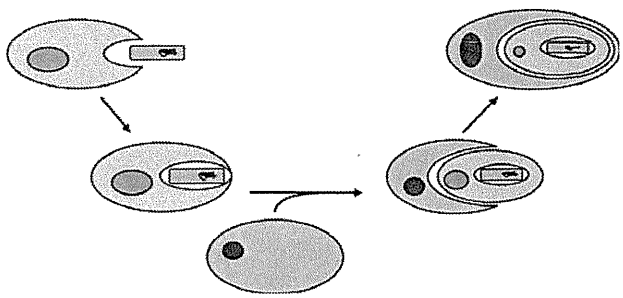

図3 アピコプラストの成立機序。通常の葉緑体は光合成細菌（緑）が植物の祖先（ピンク）に取り込まれて進化したものとされているが、アピコプラストは光合成細菌を取り込んだ紅藻類の祖先が原虫の祖先生物（紫）に取り込まれることによって成立したと考えられている。

須のオルガネラである [10]。しかしながらその機能の詳細は不明であり，何故原虫の生存に必須なのかもはっきりとはわかっていない。いずれにしても，アピコンプレクス門原虫の細胞内には植物が「組み込まれている」ということは今やよく知られている事実となっている。

2. トキソプラズマ

アピコンプレクス門に属するトキソプラズマは，ほとんどの温血動物の全ての有核細胞に感染能を持ち，全人類の 1/3 以上，日本人の約 25 − 30%が感染していると言われている非常に広く蔓延している寄生性原生生物である [3]。多くの感染者にとってトキソプラズマ感染は不顕性に経過するが，一方でトキソプラズマ感染症は一度発症すると非常に重篤な感染症となる。1999 年アメリカ CDC からの報告の中では，トキソプラズマ症は，food borne disease による全入院患者のうち原因の明らかになったものの 4.1%（第 4 位），死者数においては 20.7%（第 3 位）にもなると推定されている [6]。また，トキソプラズマ原虫は HIV 感染者に致死的な脳炎を引き起こして患者を死に至らしめることが知られており，アメリカでの統計によると HIV 感染患者の 18−25%がトキソプラズマ脳炎を発症することが報告されている [4]。一方 1999 年 WHO からの報告によると [13]，1998 年の全世界の総死者数の 25%を占める，感染症による死者のうち，17.3%が AIDS を原因として亡くなっている事と合わせて考えると，世界中の感染症による死者の約 4%はトキソプラズマ感染症が原因で亡くなっていると見積もることができる。

トキソプラズマが人に感染した場合，その増殖はタキゾイトとブラディゾイトという 2 つのステージに分けることができる（図 4）。タキゾイトは宿主細胞内に形成された小胞内で急速に増殖するステージで，宿主細胞内への侵入，分裂，宿主細胞からの脱出と次の宿主細胞への移動と付着を次々と繰り返し，感染を広げていく。一方，ブラディゾイト，あるいはシストと呼ばれるステージでの原虫の分裂は非常に緩慢で，シストは主に中枢神経系や筋肉系に存在している。シストとなった原虫は宿主の免疫応答から逃れ，宿主が免疫抑制状態になり再活性化できるまで長期間生存する。再活性化した原虫は再びブラディゾイトとなり感染を再拡大し，宿主の組織を破壊する。

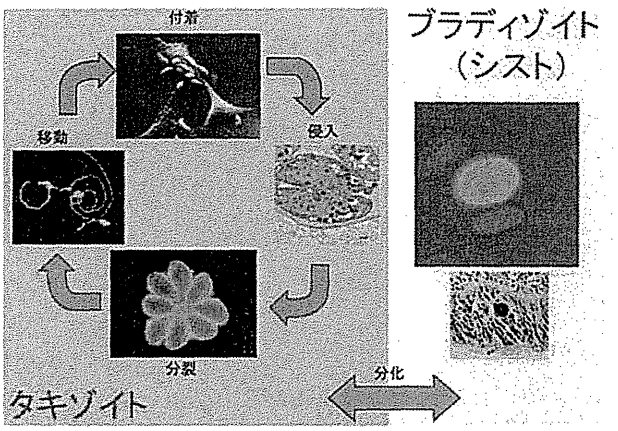

図 4　トキソプラズマの増殖サイクル。宿主に感染したトキソプラズマは最初タキゾイトとして活発に増殖する。その後、原虫は増殖をほとんど停止し、宿主からの免疫応答から逃れるため被嚢したブラディゾイト（シスト）へと分化し、再活性化の機会を待つ。

3. トキソプラズマと植物ホルモン

著者らは最近，トキソプラズマが植物ホルモンの一種であるアブシジン酸を産生し，原虫はこのホルモンにより自身の増殖を調節していることを見出した [8]。アブシジン酸は高等植物ではセカンドメッセンジャーである cyclic ADP−robose (cADPR) の産生依存的に細胞質内へのカルシウム放出を引き起こすことが知られている。このアブシジン酸をトキソプラズマに添加すると，原虫の運動や宿主細胞への侵入に重要な役割を持つマイクロネームタンパク質の分泌が誘導された。著者らは既に，マイクロネームタンパク質の分泌は cADPR 依存的な原虫細胞質内カルシウム濃度の上昇に依存していることを見出していたので [2]，実際にアブシジン酸添加後に原虫の産生する cADPR を測定したところ，加えたアブシジン酸量に依存して有意に上昇していた。また，このアブシジン酸によるマイクロネームタンパク質分泌は細胞質内カルシウム濃度の上昇に依存していることが確認できた。

更に我々は MS 解析により，トキソプラズマ原虫が実際にアブシジン酸を産生していることを証明した。また，宿主細胞内の原虫に外部からアブシジン酸を加えると，原虫の宿主細胞からの脱出が誘導さ

れた。更に，植物においてアブシジン酸生合成の特異的阻害剤であることが知られているフルリドンは，トキソプラズマにおいてもアブシジン酸生合成を阻害した。そこで原虫の培養をフルリドン処理すると，トキソプラズマは加えたフルリドンの濃度依存的に宿主細胞からの脱出が阻害された。またこの阻害は外部からのアブシジン酸添加によって相補できた。これらのことからアブシジン酸は原虫にとって，宿主細胞からの脱出のシグナルになっていると思われた。また，アブシジン酸生合成阻害剤フルリドンの培養中への添加によりアブシジン酸の生合成を阻害すると，原虫のシストへの分化が誘導された。以上の結果から，トキソプラズマ原虫はアブシジン酸を産生しており，アブシジン酸は原虫内でカルシウム放出のセカンドメッセンジャーであるcADPR産生を誘導し，細胞質内カルシウム濃度を上昇させ，宿主細胞からの脱出やそれに伴う運動と次の宿主細胞への侵入を促進する，また一方でアブシジン酸の濃度の減少は原虫のシストへの分化を誘導する，という一連のシグナルの存在が示唆された（図5）。

フルリドンは一方で，マウスを用いたトキソプラズマ感染実験において，マウスの致死率を有意に減少させた。フルリドンが哺乳動物に対し毒性が弱く，除草剤として用いられている事実と合わせて考えると，この結果は，フルリドン，あるいはアブシジン酸生合成阻害剤は抗トキソプラズマ薬開発のいいリード化合物となる可能性が示唆された。

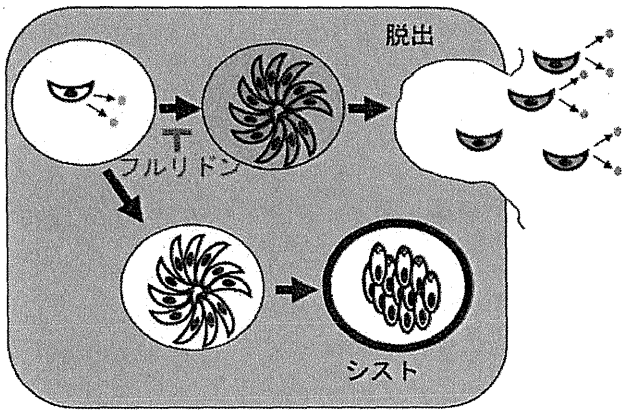

図5　トキソプラズマが産生する植物ホルモン、アブシジン酸の作用機序。アブシジン酸（オレンジ）の蓄積が原虫細胞質内カルシウム（青）濃度の上昇を引き起こし、原虫は宿主細胞からの脱出やマイクロネームタンパク質（緑）の分泌を開始する。フルリドンはアブシジン酸の生合成を阻害し、原虫の脱出を抑制することによりシストへの分化を誘導する。

4. おわりに

マラリア原虫やトキソプラズマを初めとする，多くのアピコンプレクス門原虫はアピコプラストと呼ばれる紅藻由来の共生器官を持っていることから，これらアピコンプレクス門原虫は葉緑体由来の多くの代謝経路を未だ保持している可能性が考えられている。事実，アピコンプレクス門原虫はイソプレノイドを合成するための経路（メバロチン経路）を消失しており，そのためイソプレノイド合成は，植物と同じDOXP-MEP経路を持つアピコプラストに依存していることが知られている[11]。高等植物において，アブシジン酸の生合成の多くのステップは葉緑体内で行われていることと，アブシジン酸生合成はイソプレノイドからβ-カロチンを合成することから開始されることから，おそらくトキソプラズマにおいてもアブシジン酸生合成の大部分はアピコプラストにおいて行われている可能性が示唆できる。また，アピコンプレクス門原虫において既に光合成能を失ったアピコプラストが未だ原虫の生存に必須であるという理由の一つに，今回見出されたアブシジン酸生合成経路の存在があるのかもしれない。さらにアピコンプレクス門原虫が，その進化の過程でアブシジン酸生合成経路のみを保存し活用してきたとは考えにくい。トキソプラズマを始めとするアピコンプレクス門原虫が，アブシジン酸以外の他の植物ホルモンを産生している可能性は充分考えられる。

参考文献

1. Archibald, J. M. and Keeling, P. J. 2002. Recycled plastids: a 'green movement' in eukaryotic evolution. *Trends Genet.* **18**: 577-584.
2. Chini, E. N., Nagamune, K., Wetzel, D. M. and Sibley, L.D. 2005. Evidence that the cADPR signalling pathway controls calcium-mediated microneme secretion in *Toxoplasma gondii*. *Biochem. J.* **389**: 269-277.
3. Dubey, J. P. 2007. The histology and life cycle of

Toxoplasma gondii. pp. 1−17. *In* : Toxoplasma gondii, (Weiss, L.M. and Kim, K. eds.) Academic Press.

4. Kasper, L. H. and Buzoni−Gatel, D. 1998. Some opportunistic parasitic infections in AIDS: Candidiasis, Pneumocystosis, Cryptosporidiosis, Toxoplasmosis. *Parasitol Today.* **14** : 150−156.
5. Levine, N.D. 1988. The Protozoan Phylum Apicomplexa, CRC Press.
6. Mead, P. S., Slutsker, L., Dietz, V., McCaig, L. F., Bresee, J. S., Shapiro, C., Griffin, P. M. and Tauxe, R. V. 1999. Food−related illness and death in the United States. *Emerg. Infect. Dis.* **5** : 607−625.
7. Moore, R. B., Obornik, M., Janouskovec, J., Chrudimsky, T., Vancova, M., Green, D. H., Wright, S. W., Bolch, C. J., Heimann, K., Slapeta, J., Hoegh−Guldgerg, O., Logsdon, J. M. and Carter, D.A. 2008. A photosynthetic alveolate closely related to apicomplexan parasites. *Nature.* **451** : 959−963.
8. Nagamune, K., Hicks, L. M., Fux, B., Brossier, F., Chini, E. N. and Sibley, L. D. 2008. Abscisic acid controls calcium−dependent egress and development in *Toxoplasma gondii*. *Nature.* **451** : 207−210.
9. Okamoto, N. and McFadden, G. 2008. The mother of all parasites. *Future Microbiol.* **3** : 391−395.
10. Ralph, S. A., van Dooren, G.G., Waller, R. F., Crawford, M. J., Fraunholz, M. J., Foth, B. J., Tonkin, C. J., Roos D. S. and McFadden, G.I. 2004. Tropical infectious diseases: metabolic maps and functions of the *Plasmodium falciparum* apicoplast. *Nat. Rev. Microbiol.* **2** : 203−216.
11. Sibley L. D. 2004. Intracellular parasite invasion strategies. *Science.* **304** : 248−253
12. Wellems, T. E., Hayton, K. and Fairhurst, R. M. 2009. The impact of malaria parasitism: from corpuscles to communities. *J. Ciln. Invest.* **119** : 2496−2505.
13. WHO 1999. World Health Organization Report on Infectious Diseases : Removing obstacles to healthy development.

編 集 後 記

春光うららかな季節となりました。皆様におかれましてはいかがお過ごしでしょうか。

さて今年度の編集委員で行ってまいりました編集作業も，今号を持って終了致します。不慣れな点から行き届かない部分が多々ありましたことを，この場をお借りし深くお詫び申し上げます。次年度は，「堤 信幸」「大嶋 篤」「山下 龍」が編集を担当致します。読者の皆様におかれましては，季節柄どうかご自愛ください。今後とも，引き続き日生研たよりを御愛読賜りますよう，宜しくお願い申し上げます。

（編集委員長）

NIBS

——テーマは「生命の連鎖」——
生命の「共生・調和」を理念とし，生命体の豊かな明日と，研究の永続性を願う気持ちを快いリズムに整え，視覚化したものです。カラーは生命の源，水を表す「青」としています。

表紙題字は故中村稔治博士の揮毫

日生研たより　昭和30年9月1日創刊(隔月1回発行)
(通巻573号)　平成24年2月25日印刷　平成24年3月1日発行(第58巻第2号)
発行所　財団法人 日本生物科学研究所
〒198-0024　東京都青梅市新町9丁目2221番地の1
TEL：0428(33)1056(企画学術部)　FAX：0428(33)1036
発行人　林　志鋒
編集室　委　員／平　修(委員長)，堤 信幸，黒田 丹
事　務／企画学術部
印刷所　株式会社 精興社

小さくてか弱くて臆病で歩くのがへたっぴなドジっ子ちゃん。
でも本当はとてもしたたかで驚くほど凶悪な一面を持っている。
その蠱惑的なギャップがもう、たまらない。

Toxoplasma gondii　～三日月に恋してる～

福士路花・松原立真・永宗喜三郎
国立感染症研究所寄生動物部, 筑波大学大学院生命環境科学研究科,

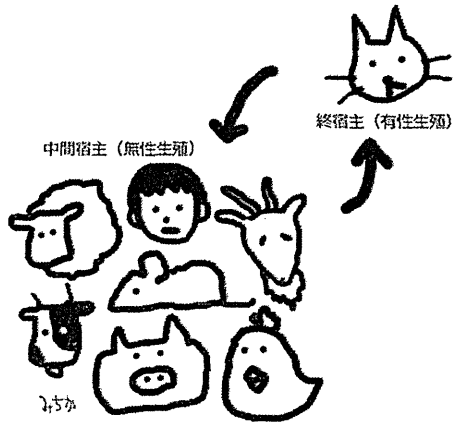

図１：トキソプラズマの生活環

トキソプラズマは寄生虫である。
ネコ科生物の中で有性生殖を行い、ヒトを含む様々な温血動物の体内で無性生殖を行う(図１)。

ヒトや家畜に感染し病気を引き起こす点や、培養の容易さから、トキソプラズマの分子生物学的研究の多くが無性生殖期を使って行われている。我々もご多分に漏れず無性生殖期を扱っているのだが、無性生殖期だけを取り上げてみてもトキソプラズマは十二分に面白い。そしてカワイイ。

無性生殖期のトキソプラズマには急増虫体と緩増虫体がある。急増虫体は名前の通りどんどん分裂して数を増やす。そのうち宿主細胞の免疫系に認識され攻撃を受けると、シスト壁を被った緩増虫体になり筋細胞や神経細胞などに潜り込み、宿主の免疫系が弱る日までおとなしく隠れている。とても臆病な、ザ・日和見感染である。

本稿では、みなさまにトキソプラズマを知って貰うため、独断と偏見で選んだ３つのチャームポイントをご紹介したい。

●チャームポイント１　～どんくさい～

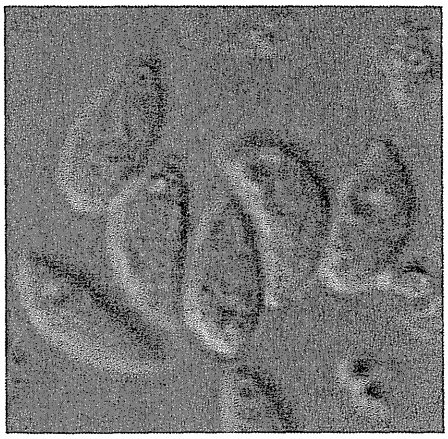

図２：無性増殖虫体

無性生殖期のトキソプラズマは、ころりとふとった三日月型で、タテ×ヨコは７ μm×３ μm 程である(図２)。鞭毛や繊毛といった運動のための構造はなく、代わりに細胞骨格と細胞膜タンパクが繋がった複雑な構造体を形成し、それをカヌーのオールのように使って運動している[1]。この通りシステムは立派だが、いかんせん、どんくさい。顕微鏡でトキソプラズマを見ていると、皆目的地も定まらずモゾモゾと身をくねらせ、時折その場でエイヤと回転するばかりで、まともに直進しているものは殆どいない。たまに立ち上がってこちらに向かってエグザイルばりの回転をするものもいる。この運動様式は様々な論文で報告されているが[2]、何の為に行われているのかは不明である。もしかして、私に向かってなにかを訴えているのだろうか。

●チャームポイント２　～宿主を操るしたたかさ～

そんなどんくさいトキソプラズマだが、宿主細胞に入る時はにゅるんとなめらかに滑り込んでゆく。トキソプラズマは宿主細胞膜を突き破るのではなく、まるで貪食されているかのように、宿主細胞膜を押しながら自身を包む“寄生胞”を形成し細胞質内に侵入する。そしてその寄生胞の中で、一体誰に教わったのか、美しいロゼッタ模様を描きながら増えていく(図 3)。増えに増えた最後は宿主細胞を破り捨て、再び新たな寄生先を見つけるために飛び出していく。

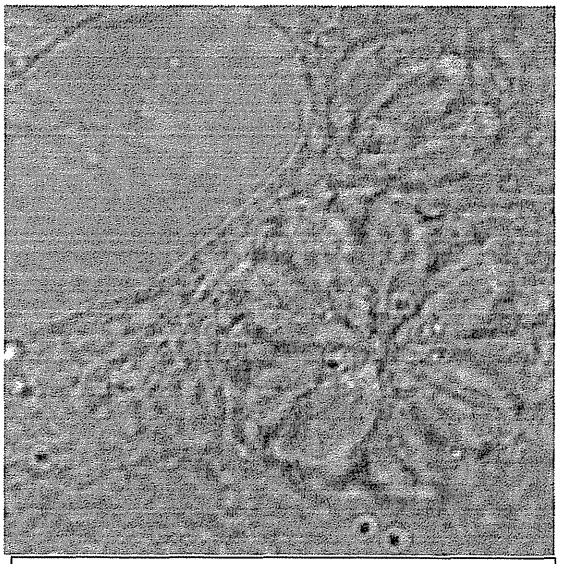

図３：宿主細胞中のトキソプラズマ
右下に大きい寄生胞(16 虫体)が、右上に小さい寄生胞(4 虫体)が見える。エンドダイオジェニーという特殊な分裂様式をとるために、お花型になって増えていく。左上は宿主核。
なんらかの嗜好があるらしく、このように人気のある物件（宿主細胞)と誰にも入って貰えない不人気な物件がある。

侵入直前から侵入後宿主細胞質内にいる間、トキソプラズマは様々なタンパク質を分泌して宿主細胞をコントロールする。具体的には、宿主細胞の転写因子をリン酸化して免疫系機能をコントロールしたり、分解を防ぐために宿主のリソソームを遠ざけたり、逆に宿主の ER(小胞体)やミトコンドリアを寄生胞の周りに引き寄せている(図 4)。

免疫系のコントロールメカニズムは近年続々と新しい報告が上がっているが[3][4]、オルガネラ引き寄せのメカニズムについては未だ核心を突く発見はなされていない。そもそも、これらのオルガネラが通常宿主細胞の中でどのように動いているのかもきちんとわかっていない。つまりトキソプラズマの宿主オルガネラ引き寄せメカニズムの理解によって、宿主細胞のオルガネラ運動の原理も解明できるかもしれない、という一石二鳥なロマン溢れる可能性が秘められている。ちなみに、引き寄せた宿主の ER やミトコンドリアから何を得ているのか、あるいは何をさせているのかもよくわかっていない。原生動物園第２巻には“原生動物の最大の特徴は「食べる」ことです”とあるが、トキソ

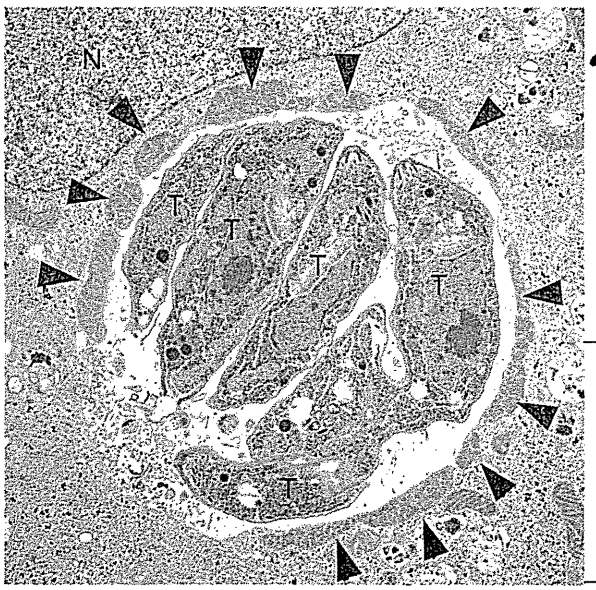

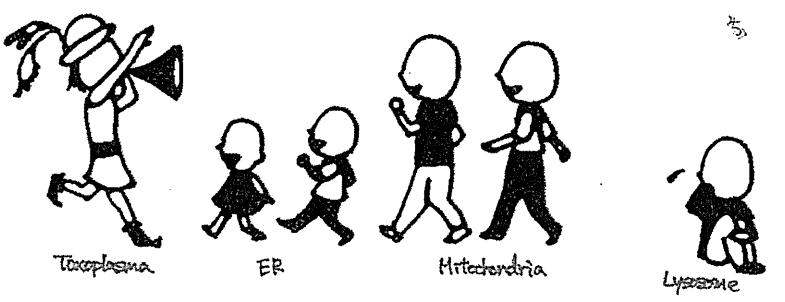

図 4：左図は宿主細胞中のトキソプラズマ。トキソプラズマ(T)を含む寄生胞の周りに宿主のミトコンドリア(▲)が引き寄せされている。N は宿主核を示す。
右図は宿主細胞オルガネラの引き寄せイメージ図。

プラズマにおいてはその限りではなく、今のところ貪食をするという報告はない（ピノサイトーシスは行うと考えられる）。しかし彼らが持つ分泌器官の１つは、かつてミゾサイトーシスという、相手細胞の中身をジュルジュルと吸い取るという若干気色悪い摂食様式を行うための捕食器官だったといわれている[5][6]。...もしかしたら、私の父が夜中に時々冷蔵庫を漁っているように、実は我々の目を盗んで時々こっそり宿主をジュルジュルやっているのかもしれない。そう思いたくなるほど彼らの体型はよく似ている。

またトキソプラズマは細胞だけではなく、個体レベルでも宿主をコントロールしているといわれている。具体的な例として、トキソプラズマに感染したマウスはネコの尿に対する忌避反応が低下することが知られている[7]。これはマウスをネコに捕食されやすくすることで感染サイクル成立の効率を上げる効果があると考えられている。人間においても、トキソプラズマに感染すると性格が変わったり、精神疾患や自殺のリスクが高まったり、サッカーが強くなったり[8]、交通事故に遭いやすくなったりする、というオカルティックな報告がいくつか挙げられているが、このあたりの信憑性は定かではない。ただし、トキソプラズマは神経細胞に好んで潜伏感染することや、ドーパミン様物質の産生を行うことから、一概に胡散臭いと一蹴もできない。かもしれない。

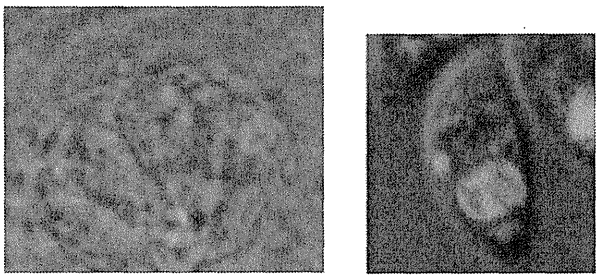

図５：(左) 赤色蛍光染色したアピコプラスト (taken by S. B. A. Andrabi)
(右) 青色蛍光染色した核、大きいのがトキソプラズマの核で、小さいのがアピコプラストの核。わずか 35kb とは思えない存在感である。

●チャームポイント３　～謎めいた過去～

花が咲くように可憐な姿で増殖するトキソプラズマだが(図 3)、姿だけではなく分子メカニズムにおいても植物的要素を持っている。光合成しないのに植物ホルモンを使用するのである[9]。この原生動物園第２巻でも取り上げられているが、トキソプラズマにはアピコプラストと呼ばれる二次共生色素体が存在する(図 5)。これは遠い昔に紅藻類をとりこんで獲得したものだと考えられており、恐らく当初は光合成のために使用していたが、長い時を経てその能力を失い、現在は脂質合成の場として利用されている[10]。一体トキソプラズマが寄生するようになったために光合成能が失われたのか、それともアピコプラストが光合成能を失ったためにトキソプラズマは寄生生活を強いられたのか(図 6)、それは依然謎である。

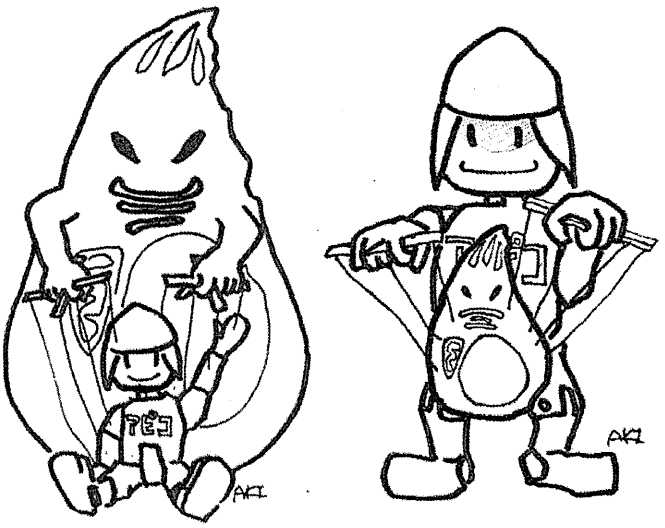

図６：トキソプラズマとアピコプラスト、どちらが操られているのか？ (drawn by A. Yamano)
興味を持った方は新学術領域マトリョーシカ型進化原理[13]も合わせてご覧下さい。

アピコプラストを獲得したことで、トキソプラズマは植物ホルモンを産生し、自身の細胞分裂や分化の制御に使用する様になったと考えられている[11]。ただし、今のところ植物ホルモ

ン合成に携わる器官や酵素などはきちんと解明されていない。現在植物で使われているような酵素のオルソログなども見つかっておらず、このあたりの合成経路などが解明されれば、植物ホルモン分野においても新しい知見をもたらすことができるという一石二鳥なロマン溢れる可能性が秘められている（デジャヴではない）。

またアピコプラストの他にも、近年発見されたPLV (Plant-Like Vacuole)と呼ばれる植物の液胞のようなオルガネラを持つことも分かっている[12]。このオルガネラは宿主細胞の外に出た時にしか形成されず、侵入後になくなる。そんなもの作ってるヒマがあったらさっさと宿主に侵入すれば良いのに。不思議ちゃんである。

このように植物的でありながら、宿主に能動的に入り込んで骨の髄までしゃぶり尽くすこの肉食ぶり。まさにロールキャベツ系。

この他トキソプラズマが持つ魅力的な謎は数え上げればきりがない。殆どの寄生虫（単細胞・多細胞共に）は宿主域が非常に狭く、種レベルで宿主を限定する生物も少なくない中で、なぜトキソプラズマは様々な中間宿主に感染できるのか。そもそもなぜ寄生というメンドくさい生き方になったのか。今後どうなるのか－ずっとこのままなのか、更に病原性を高めるのか、それとも共生への道を進むのか？

トキソプラズマは医学的、獣医学的には勿論だが、分子生物学的、進化学的にも非常に面白い謎を提供してくれている、まさに一粒で３度も４度もおいしい生物である。しかもかわいい。なんともたまらん生物である。

Acknowledgement

原生動物園という画期的な試みに、原稿執筆のチャンスを下さった早川昌志氏に心よりお礼申し上げます。また、この文章を書くにあたりラボメンバーに大きな協力を頂きました。この場を借りてお礼申し上げます。

ちなみにトキソプラズマは、最も病原性の強い株だと一匹でマウスを死に至らしめることができる。一人じゃ何も出来ない私とは大違いである。

女性必読！トキソプラズマ感染と妊娠へのリスク

健常な成人がトキソプラズマに感染した場合、殆どが無症状、あるいは風邪に似た軽微な症状がでる程度であまり問題にはなりません。しかし女性が妊娠中に初めて感染すると、胎児も感染することがあり流産や水頭症など先天性障害を引き起こす可能性があります。妊娠前のブライダルチェックや、妊娠後の健診などでトキソプラズマ感染の有無をチェックしましょう。

→詳しくはトーチの会 (http://toxo-cmv.org/) または感染研 HP (http://www.nih.go.jp/niid/ja/diseases/ta/toxoplasma.html)をご覧下さい。